Journal of Cellular Biochemistry 102:224–239 (2007)

Transitional CpG Methylation Between Promoters and Retroelements of Tissue-Specific Genes During Human Mesenchymal Cell Differentiation

Moo-Il Kang,[1] Hye-Soo Kim,[1] Yu-Chae Jung,[2] Young-Ho Kim,[2] Seung-Jin Hong,[2] Mi-Kyoung Kim,[1] Ki-Hyun Baek,[1] Chun–Choo Kim,[1] and Mun-Gan Rhyu[2]*

[1]Department of Internal Medicine, College of Medicine, The Catholic University of Korea, Seoul, Korea
[2]Department of Microbiology, College of Medicine, The Catholic University of Korea, Seoul, Korea

Abstract In general, methylation of the promoter regions is inversely correlated with gene expression. The transitional CpG area between the promoter-associated CpG islands and the nearby retroelements is often methylated in a tissue-specific manner. This study analyzed the relationship between gene expression and the methylation of the transitional CpGs in two human stromal cells derived from the bone marrow (BMSC) and adipose tissue (ATSC), both of which have a multilineage differentiation potential. The transitional CpGs of the osteoblast-specific (RUNX2 and BGLAP), adipocyte-specific (PPARγ2), housekeeping (CDKN2A and MLH1), and mesenchyme-unrelated (RUNX3) genes were examined by methylation-specific PCR. The expression of each gene was measured using reverse-transcription PCR analysis. The RUNX2, BGLAP, and CDKN2A genes in the BMSC, and the PPARγ2 gene in the ATSC exhibited hypomethylation of the transitional CpGs along with the strong expression. The CpG island of RUNX3 gene not expressed in both BMSC and ATSC was hypermethylated. Transitional hypomethylation of the MLH1 gene was accompanied by the higher expression in the BMSC than in the ATSC. The weakly methylated CpGs of the PPARγ2 gene in the BMSC became hypomethylated along with the strong expression during the osteoblastic differentiation. There were no notable changes in the transitional methylation and expression of the genes other than PPARγ2 after the differentiation. Therefore, the transitional methylation and gene expression established in mesenchymal cells tend to be consistently preserved under the induction of differentiation. Weak transitional methylation of the PPARγ2 gene in the BMSC suggests a methylation-dependent mechanism underlying the adiopogenesis of bone marrow. J. Cell. Biochem. 102: 224–239, 2007.

Key words: methylation; mRNA expression; cell differentiation; mesenchymal cell

Stromal cells derived from bone marrow (BMSC) and adipose tissue (ATSC) can proliferate easily and differentiate in vitro into a variety of cell lineages such as osteoblasts, chondrocytes, adipocytes, and myoblasts [Kern et al., 2006]. These two mesenchymal cells are considered promising resources for stem cell therapy in the regeneration of tissue with a mesenchymal origin. Currently, it is not known if this multi-lineage potential produces separate precursor cells that exist in vivo, or if the stem cell potential emerges in the in vitro culture conditions. In contrast, it has been suggested that mesenchymal cells are inherently unstable and shift from one lineage to another [Dennis and Charbord, 2002]. For example, the aging process, which is one of the causes of osteoporosis, is associated with the increased adipogenesis and decreased osteogenesis of mesenchymal cells in the bone marrow. Eventually, the red marrow turns yellow and the differentiation capacity of the BMSC in elderly people becomes inefficient [Justesen et al., 2001; Pei and Tontonoz, 2004].

The RUNX2 [Komori et al., 1997; Otto et al., 1997] and PPARγ2 [Ross et al., 1990; Tontonoz et al., 1994] genes are well-known "master

Moo-Il Kang and Hye-Soo Kim have contributed equally to this work.

Grant sponsor: The Ministry of Health & Welfare, Republic of Korea; Grant number: 0405-DB01-0104-0006.

*Correspondence to: Mun-Gan Rhyu, MD, PhD, Department of Microbiology, College of Medicine, The Catholic University of Korea, 505 Banpo-dong, Socho-gu, Seoul 137-701, Korea. E-mail: rhyumung@catholic.ac.kr

Received 21 August 2006; Accepted 9 January 2007

DOI 10.1002/jcb.21291

genes" that drive the osteoblastic and adipocytic differentiation of mesenchymal cells, respectively. Generally, it is believed that the specification of the cell lineage is established based on a cell-intrinsic epigenetic program that guides genome-wide DNA methylation during mammalian embryogenesis and development [Holliday and Pugh, 1975]. Individual embryonic cells reconstruct new methylation marks after initial genome-wide demethylation, which separates the embryo with high-level methylation from the placenta with low-level methylation [Reik et al., 2001]. Postnatal increases and decreases in methylated CpGs of certain DNA sequences have been detected in specific tissues, suggesting that the methylation-variable CpGs are associated with somatic cell differentiation [Shiota, 2004]. Therefore, it is important to determine if a methylation-dependent mechanism is involved in the expression of the mesenchyme-related genes as well as the differentiation of mesenchymal cells toward multiple lineages.

Binding motifs for transcription factors usually overlap with a CpG-rich island, which ensures easy access to the transcription factors [Bird, 1986; Larsen et al., 1992]. The *Alu* and L1 retroelements, which are highly repetitive sequences that are distributed throughout the human genome, elicit the spread of CpG methylation into nearby genomic sequences [Hata and Sakaki, 1997; Yates et al., 1999; Arnaud et al., 2000]. Although the CpG islands are consistently unmethylated in most tissue types, some transitional CpG sites between retroelements and promoters are methylated to various levels in a tissue-specific manner [Kang et al., 2006]. Methylation-variable CpGs associated with the retroelements could be found near the boundaries of CpG islands and at the nonisland CpG sites close to the transcription start sites of the genes lacking CpG islands [Kang et al., 2006; Kim et al., 2006], which are expected to influence the phenotype plasticity of mesenchymal cells through the DNA methylation-dependent mechanism.

Tissue-specific transitional methylation between the transcription start site and the nearest retroelements was previously described for the mesenchyme-related (RUNX2) and -unrelated (RUNX3) genes as well as the housekeeping genes (CDKN2A and MLH1) [Kang et al., 2006; Kim et al., 2006]. This study examined tissue-specific transitional methylation and gene expression in the BMSC and ATSC under the differentiation induction and oxidative stress. The transitional CpG sites of the mesenchyme-related genes (RUNX2, BGLAP, and PPARγ2) were completely hypomethylated along with the increased gene expression. Interestingly, the transitional CpGs of the PPARγ2 gene that were weakly methylated in the BMSC were completely hypomethylated under the osteogenic induction and oxidative stress in agreement with a propensity of the bone marrow to undergo adipogenesis.

MATERIALS AND METHODS

Preparation of Primary Cells

Bone marrow specimens were diluted with an equal volume of α-minimum essential medium (α-MEM) and were layered carefully on Ficoll-Hypaque. The cell pellets obtained by density-gradient centrifugation were suspended in a standard α-MEM medium containing 10% fetal bovine serum (FBS), and were plated at 4×10^5 nucleated cells/ml. The adipose tissue obtained during abdominal surgery was minced and digested with 0.1% collagenase for 40 min at 37°C. The tissue-collagense mixture was diluted with a twofold volume of a standard α-MEM medium, and centrifuged for 10 min. The supernatant containing the lipid droplets was discarded. The cells that settled at the bottom were collected with the standard α-MEM medium. The Institutional Review Board approved this study, and written informed consent was obtained from each person prior to the study.

Stromal cells derived from bone marrow and adipose tissue were culture-expanded for a total of 4–5 weeks. When the culture dishes were almost confluent, the cultured cells were detached using trypsin, plated at 5×10^4 cells/ml in 75 cm^2 T-flasks, and nourished with a standard medium for 3 days. The primary cultures were then grown under the following three different conditions: control, differentiation induction, and H_2O_2 treatment.

Differentiation Induction and Oxidative Stress

For the differentiation induction, the attached cells were grown with the osteogenic supplements (0.1 μM dexamethasone, 10 mM β-glycerophosphate, and 50 μg/ml ascorbic acid) or adipogenic supplements (1 μM dexamethasone,

10 μM insulin, 200 μM indomethacin, and 0.5 mM isobutyl-methylxanthine) for a further 2 weeks. The histochemical stain for alkaline phosphatase was carried out to check the level of osteogenic differentiation. The cells were fixed in 4% paraformaldehyde and 0.2 M cacodylic acid for 10 min at 4°C, and incubated with an ALP solution (Sigma, St. Louis, MO, USA) for 1 h at 37°C. Cells stained with pink cytoplasm indicated the alkaline phosphatase activity. An intracellular lipid droplet in the adipogenic media was stained with Oil Red O. The cells were fixed in 60% isopropyl alcohol for 10 min and incubated in 2% Oil Red O reagent (Sigma) for 10 min at room temperature. The stained cells showed cytoplasmic red vacuoles.

The BMSC and ATSC were grown in a standard α-MEM medium until they had reached 50% confluence and were treated with H_2O_2 at a concentration of 0, 0.1, 0.3, and 0.5 mM in a standard medium without FBS for 24 h. The cells were then grown in standard α-MEM medium including 10% FBS for 7 days. The cells from each group were harvested and frozen at −70°C to evaluate the level of DNA methylation and mRNA expression.

DNA Modification by Sodium Bisulfite

Ninety microliters of the genomic DNA (20 ng/μl) was denatured with 10 μl of 3 M NaOH for 15 min at 37°C prior to sodium bisulfite modification. For sodium bisulfite modification, 100 μl of the denatured DNA was treated with 1,040 μl of 2.3 M sodium bisulfite and 60 μl of 10 mM hydroquinone for 12 h at 50°C. The modified DNA was purified using Wizard DNA purification resin (Promega, Madison, WI, USA), precipitated with ethanol, and dissolved in 35 μl of a 5 mM Tris buffer (pH 8.0). One microliter aliquot of the modified DNA solution was placed in a PCR tube and stored at −20°C.

Methylation-Specific PCR and Sequencing of Bisulfite-Modified DNA

The coding and noncoding sequence information for the RUNX2, BGLAP, PPARγ2, CDKN2A, MLH1, and RUNX3 genes was obtained from the human genome database (http://genome.ucsc.edu). The genomic locations and annotations of the retroelements were derived from the RepeatMasker program output (http://ftp.genome.washington.edu/RM/RepeatMasker.html) based on RepBase [Jurka, 2000]. A CpG island was defined as a DNA segment with a G+C content ≥50%, longer than 200 bp nucleotides, and an Obs/Exp CpG ratio over 0.6 [Gardiner-Garden and Frommer, 1987]. The methylation-specific PCR (MSP) primers of the six genes were designed between promoters and retroelements, as shown in Figure 1 and Tables I and II.

The methylation status of the transitional CpGs was estimated using the semiquantitative MSP protocol reported elsewhere [Hong et al., 2005; Kang et al., 2006]. MSP analysis was performed in a minimum number of amplification rounds for sub-plateau DNA amplification using the radioisotope. The bisulfite-modified DNA was amplified and labeled by a hot-start PCR containing α-^{32}P dTTP (PerkinElmer, Boston, MA, USA) and dNTP mixture through 32 PCR cycles. The PCR products were loaded onto a nondenaturing polyacrylamide gel and visualized by repeated autoradiography using a radioluminograph scanner (BAS 2500, Fuji Photo Film, Kanakawa, Japan). The high specificity of each MSP primer set was validated using the universal methylated and unmethylated DNAs. The amplification intensity of the methylation and unmethylation primer sets increased linearly with increasing percentage of the control DNA in the MSP template-primer mixtures. The methylation density was calculated from the relative proportion of a methylation band in the combined total of methylation and unmethylation band intensities. All MSP experiments were performed using three independent samples and each experiment was repeated twice to confirm the same result.

The number and position of methylated CpGs in the transitional area were examined by cloning and sequencing the common PCR DNA as described previously [Hong et al., 2005; Kang et al., 2006; Kim et al., 2006]. The methylation-variable CpGs were further methylated in the distal portion of the CpG amplicon. For example, the CpG amplicons of the RUNX2, PPARγ2, and CDKN2A genes spanned the methylated distal CpGs and the unmethylated proximal CpGs (Fig. 2). The BGLAP gene showed the gradual DNA methylation in the proximity of the transcription start site. However, the intensity of the MSP bands was found to plausibly represent a difference in the status of methylation-variable CpGs between the BMSC and ATSC.

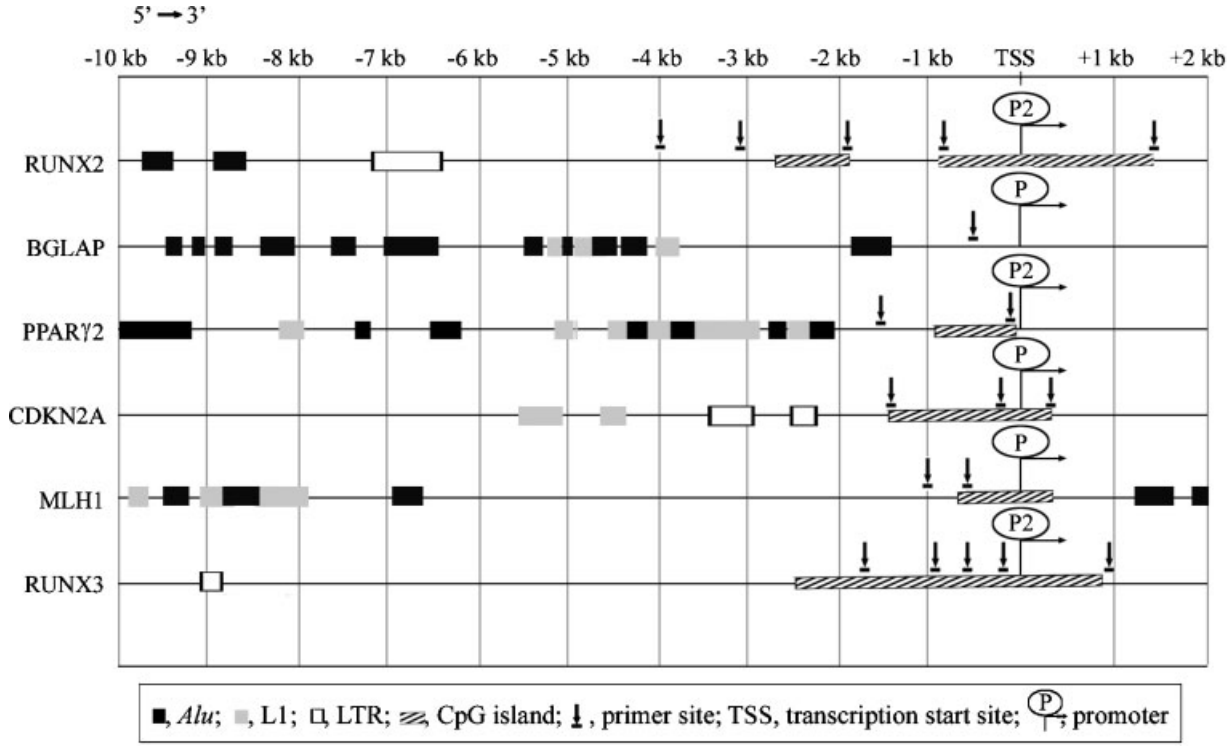

Fig. 1. Schematic diagram of the coverage of the CpG islands and the retroelement distributions in the 5′-end regions of the six genes examined by methylation-specific PCR analysis. The five genes with CpG islands were examined using more than one PCR primer set spanning the CpG island and the nonisland CpGs between the transcription start sites and the retroelements. The P2 promoters of the RUNX2, PPARγ2, and RUNX3 genes expressing two isoforms [Zhu et al., 1995; Bangsow et al., 2001; Xiao et al., 2003] overlap with the CpG islands. The BGLAP gene without a CpG island was examined at the proximal CpG site to the transcription start site.

TABLE I. Summary of CpG Sites and Exons Examined in Stromal Cells Derived From Bone Marrow and Adipose Tissue

Gene symbol	Gene description and RefSeq ID	Gene size (bp)	CpG island size (bp)	CpG amplicon (bp)[a] Unmethylation	CpG amplicon (bp)[a] Methylation	mRNA exons
RUNX2	Osteoblast differentiation NM_004348 (P2 promoter)	128,905	2,226	−3,883 −3,061 −1,947 −852 +1,573	−3,883 −3,061 −1,947 −850 +1,573	1–2
BGLAP	Osteocalcin precursor NM_199173	1,108	Absence	−502	−502	1–4
PPARγ2	Adipocyte differentiation NM_138711 (P2 promoter)	145,405	906	−141 −1,563	−141 −1,563	3–6
CDKN2A	Cell cycle G1 control NM_058195	26,739	1,375	−1,580 −85 +776	−1,575 −85 +775	1–2
MLH1	DNA mismatch repair gene NM_000249	57,357	1,128	−1,098 −660	−1,098 −655	9–11
RUNX3	Gastric mucosa differentiation NM_004350 (P2 promoter)	30,310	4,493	−1,790 −1,166 −559 −219 +952	−1,790 −1,166 −559 −217 +952	1–2

[a]Distance from the transcription start site of each gene.

TABLE II. Primer Sequences Used in Methylation and mRNA Analyses

Amplicon sites	Primer[a]	Forward	Reverse	Amplicon size (bp)
RUNX2, −3.8 kb	U	AGGTTTAGTTAGTTTTAGTTG	CCACTAAATACCCTAACAACA	113
	M	AGGTTTAGTTAGTTTTAGTCG	CCACTAAATACCCTAACAACG	113
−3.0 kb	U	TGTTTGAGTGTATATGAGTGGAT	TCTCTCAAATCCCACAAACAACCA	123
	M	TGTTCGAGTGTATATGAGTGGAC	TCTCTCGAATCCCACAAACGACCG	123
−1.9 kb	U	GGATTTTTTGGTTTTTTGTGGGT	CTCTAACTAAATCAATCATTACA	127
	M	GATTTTTCGGTTTTTGCGGGC	CTCTAACTAAATCGATCATTACG	126
−0.7 kb	U	GGTTTTGGAAATTGTATATGGTGT	AAACAACAAATCTCAAACCTACA	96
	M	TTTCGGAAATTGTATACGGCGC	AACAACGAATCTCGAACCTACG	93
+1.6 kb	U	GTTTGAGGGTGGGTGGTAGTTGT	ACTACCCCAAAAAATCTAAATCA	127
	M	GTTTGAGGGCGGGTGGTAGTCGC	ACTACCCCGAAAAATCTAAATCG	127
	RT	CCCCACGACAACCGCACCAT	CGCTCCGGCCCACAAATCTC	289
BGLAP, −0.5 kb	U	AGGGTAGGGTTTGAGTTGTT	AATACCTCACAATACCCCCA	86
	M	AGGGTAGGGTTTGAGTCGTC	AATACCTCGCAATACCCCCG	86
	RT	CCTGAAAGCCGATGTGGTC	CTCACACTCCTCGCCCTAT	262
PPARγ2, −1.5 kb	U	AGAAGAGAAAATTAAGGGATTT	ATAACTTACCCTTCACACAACA	117
	M	AGAAGAGAAAATTAAGGGATTC	ATAACTTACCCTTCACACGACG	117
−0.2 kb	U	GGTTAGGTTTTGTGTTTTGATGT	CCTAACTACACACTCCATCCA	111
	M	GGTTAGGTTTTGTGTTTTGACGC	CCTAACTACGCGCTCCATCCG	111
	RT	AAGACCACTCCCACTCCTTTG	GTCAGCGGACTCTGGATTCA	554
CDKN2A,−1.5 kb	U	TTGGGATTAGGTTTAGTTTTGG	CTATAAAACCCTATCAACTCACACT	130
	M	TCGGGATTAGGTTTAGTTTCG	AAACCCTATCGACTCACGCT	125
−0.1 kb	U	TGTTTATTTTTGTTTTTGTAGGTG	AAAACTCAAAACCATTCCAA	129
	M	TGTTTATTTTCGTTTCGTAGGC	AAAACTCAAAACCGTTCCGA	129
+0.8 kb	U	GTATTTTAGGAAGTTGTTGTTTGT	TTTTCTCCCCAACCTCCCAACA	101
	M	GTATTTTAGGAAGTCGTTGTTTGC	TTTTTCTCCCCAACCTCCCGACG	102
	RT	GGTTCTTGGTGACCCTCC	ACCAGCGTGTCCAGGAGG	331
MLH1, −1.0 kb	U	GATTTTAGGATTGTTGATATGAGT	AAACTACCTCCTAATCTTTATCCA	126
	M	GATTTTAGGATTGTCGATATGAGC	AACTACCTCCTAATCTTTATCCG	125
−0.6 kb	U	TTTTGATGTAGATGTTTTATTA-GGGTTGT	ACCACCTCATCATAACTACCCACACA	121
	M	ACGTAGACGTTTTATTAGGGTCGC	CCTCATCGTAACTACCCGCG	115
	RT	ACTCTTCATCAACCATCGTC	TTGTGGATTTAACCATCTCC	314
RUNX3, −1.7 kb	U	TGGGGTTAGATTTTTGTTGTTTTTT	ATAAAATCTTACAACCACCATCA	107
	M	CGGGGTTAGATTTTCGTTGTTTTTC	ATAAAATCTTACGACCACCGTCG	107
−1.1 kb	U	**TGTTAAATTGGGGATAGGT**	**AACCACAAACCACCACAACA**	151
	M	**TGTTAAATCGGGGATAGGC**	**AACCACAAACCGCCACAACG**	151
−0.5 kb	U	GATGTGTTGTATAGTTAATTGGT	TCCCCATTAAACAACCTCCA	97
	M	CGCGTCGTATAGTTAATCGGC	TCCCCGTTAAACGACCTCCG	95
−0.1kb	U	GGAAAGTAGAAGTGGTGGGGTTT	ACTAACCAAACAAACTACAAACA	128
	M	GAAAGTAGAAGCGGCGGGGTTC	ACTAACCGAACAAACTACGAACG	125
+1.0 kb	U	GTTGTTTTAATGGGAGTAGGGAT	CAAAATAAAACAAAAACACCTCA	147
	M	GTCGTTTTAATGGGAGTAGGGAC	GAAATAAAACGAAAACGCCTCG	147
	RT	AGGCATTGCGCAGCTCAGCGGAGTA	TCTGCTCCGTGCTGCCCTCGCACT	150

[a]The genomic position of each MSP primer sets is indicated with the gene symbol and the distance (kb nucleotides) from the transcription start site. Unmethylation (U), methylation (M), and reverse-transcription (RT) PCR primers were made for each gene. The bold sequences with a single underline indicate bisulfite-modified nucleotides.

Semiquantitative Reverse-Transcription PCR

The cDNA was synthesized in a 100 μl of reaction mixture containing the total RNA (1 μg), a random primer (3.2 μg), 10× PCR buffer, $MgCl_2$ (5 mM), dNTP (1.0 mM of each dATP, dGTP, dCTP, and dTTP), RNase inhibitor (50 U), and AMV reverse transcriptase (20 U). This reaction mixture was incubated at 25°C for 10 min and then at 42°C for 60 min. The cDNA (1 μl) was amplified in a 20 μl reaction mixture containing a 10× PCR buffer, $MgCl_2$ (25 mM), dNTP (2.5 mM of each dATP, dGTP, dCTP, and dTTP), the primers (10 pmol for each forward and reverse sequence primer), and *Taq* DNA polymerase (0.5 U). The primers of the genes examined were designed, as noted in Tables I and II. The RUNX2, PPARγ2, and RUNX3 genes have two promoters (upstream/distal P1 and downstream/proximal P2) that regulate the expression of two isoforms [Zhu et al., 1995; Bangsow et al., 2001; Xiao et al., 2003], of which the proximal P2 promoters overlapping with the CpG islands were examined. Each reaction was initiated in 94°C for 5 min; followed by 30 cycles of 94°C for 1 min (denaturation), 55–60°C for 1 min (annealing), 72°C for 1 min (extension); and terminated in 72°C for 10 min. The reverse-transcription PCR (RT-PCR) products were electrophoresed on a 1.5% agarose gel and visualized by ethidium bromide staining. For semiquantitative PCR, the linear range of amplification was first established with similar results being obtained from the duplicated PCR

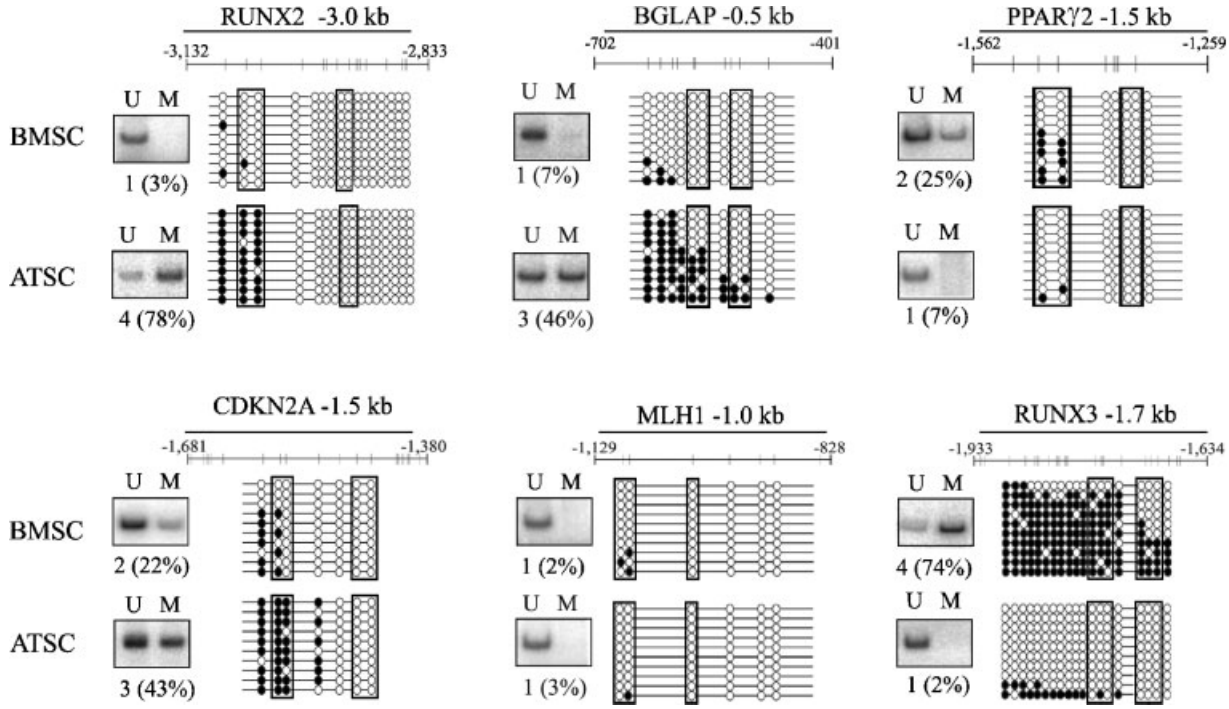

Fig. 2. Comparison of the density of methylation estimated by semiquantitative methylation-specific PCR (MSP) and sequencing of the common PCR DNA. The genomic DNA was purified from the primary cultures of undifferentiated stromal cells of bone marrow (BMSC) and adipose tissue (ATSC). The density of methylation was estimated based on the standard curve of MSP bands and is indicated below the electrophoretic lanes. The lanes marked U and M indicate the PCR bands of the unmethylated and methylated primer sets, respectively. The common primer sets encompassing the MSP primer sequences were used. The CpG sites on the MSP primers are represented in the box. The unmethylated and methylated CpG sites are shown by the open and closed circles, respectively.

reactions. The glyceraldehyde-3-phosphate dehydrogenase (GAPDH)-specific primers were used for the internal control PCR and all RT-PCR signals were normalized to this value.

RESULTS

Transitional CpG Methylation Between Transcription Start Sites and Retroelements

The transitional area between the transcription start sites and the nearby retroelements upstream of the six genes was examined using MSP analysis with the bisulfite-modified genomic DNA obtained from the BMSC and ATSC. The P2 promoter regions of the RUNX2 and RUNX3 genes containing the long CpG islands were verified using five MSP primer sets (Fig. 3A). The proximal CpG sites of the long CpG islands were consistently unmethylated in both BMSC and ATSC. There was a difference in the level of methylation of the distal CpG site, at a distance of 1.0–4.0 kb, between the BMSC and ATSC. The transitional CpGs of the PPARγ2 and CDKN2A genes were differentially methylated in the nonisland CpG sites near the promoter-associated CpG islands.

The individual variations in methylation were examined at the methylation-variable CpG sites of the RUNX2, PPARγ2, and RUNX3 genes, which contain CpG islands (Fig. 3B). Three BMSC samples were grown in the primary and secondary cultures using a standard medium. The methylation status of the methylation-variable CpG sites in a BMSC sample in the primary and secondary cultures was identical. The methylation-variable CpG site of the RUNX2 gene was completely hypomethylated in all samples and that of the PPARγ2 gene was completely or incompletely hypomethylated. The CpG island of the RUNX3 gene was completely or incompletely hypermethylated.

Transitional CpG Methylation and mRNA Expression in Mesenchymal Cells

The transitional area of each gene was examined at one methylation-variable CpG site showing the greatest difference in methylation

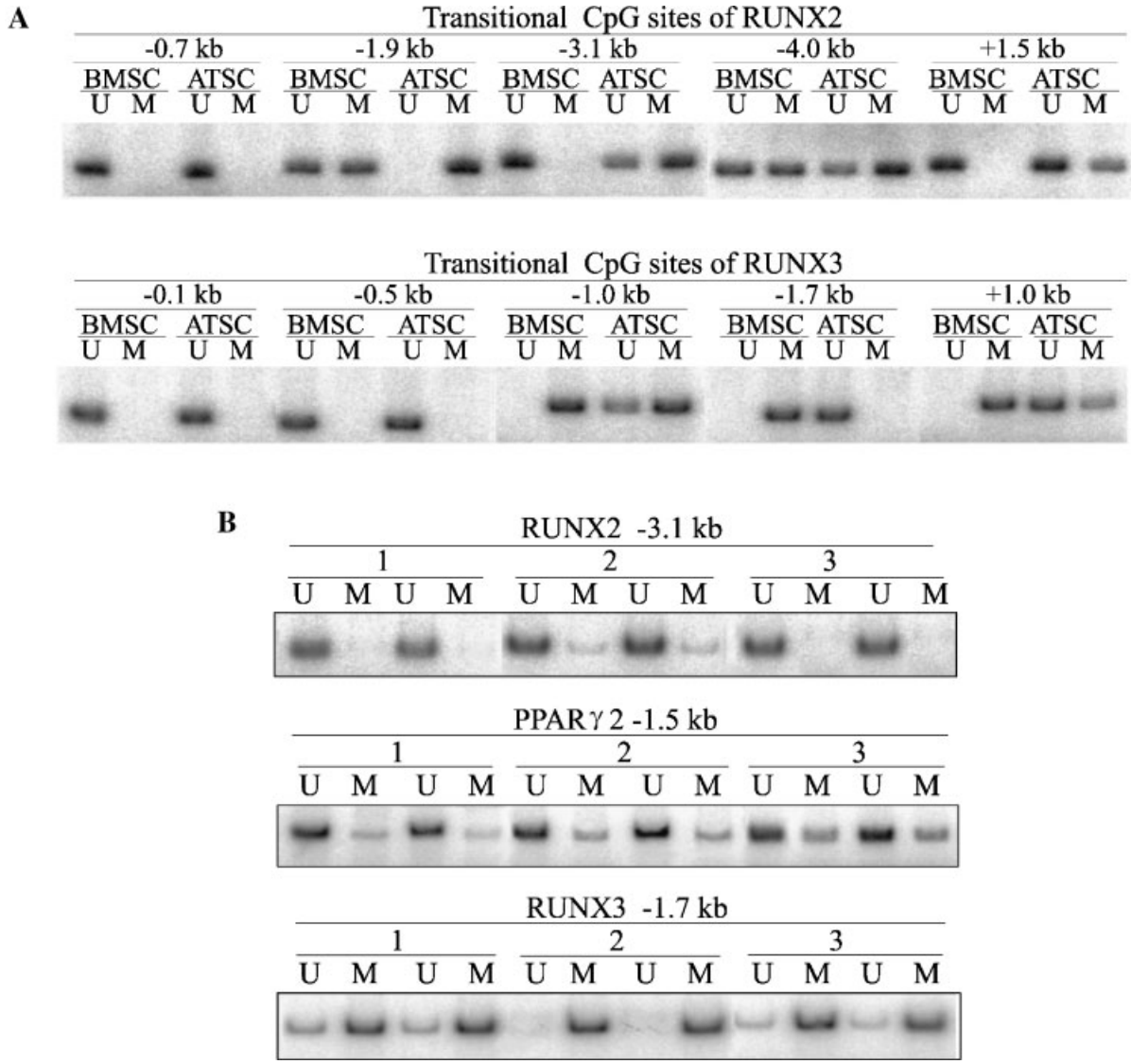

Fig. 3. The methylation status of transitional CpGs between the promoters and retroelements. The stromal cells derived from the human bone marrow (BMSC) and adipose tissue (ATSC) were examined by methylation-specific PCR using the bisulfitemodified genomic DNA and the methylation (M) and unmethylation (U) primer sets. The genomic position of each CpG amplicon is indicated by the distance (kb nucleotides) from the transcription start site. **A**: The CpG islands and nonisland CpG sites in the transitional area of the RUNX2 and RUNX3 genes were verified using five primer sets. **B**: The interindividual methylation variation was examined at the methylation-variable CpG sites of the RUNX2, PPARγ2, and RUNX3 genes. The undifferentiated BMSC was prepared from the primary and secondary cultures of three samples.

between the undifferentiated BMSC and ATSC (Fig. 4). The methylation status of the methylation-variable CpGs was divided into the following five levels: 1 (0–20%, complete hypomethylation), 2 (21–40%, incomplete hypomethylation), 3 (41–60%, intermediate methylation), 4 (61–80%, incomplete hypermethylation), and 5 (81–100%, complete hypermethylation). The level of methylation in the methylation-variable CpGs upstream of the osteoblast- (RUNX2 and BGLAP) or adipocyte-(PPARγ2) specific, cell cycle-related (CDKN2A), mismatch repair (MLH1), and stomach-specific (RUNX3) genes in the undifferentiated BMSC and ATSC were compared (Fig. 4A). A difference in methylation of more than one level between the BMSC and ATSC was observed in every gene except for MLH1. The methylation-variable CpG sites of the RUNX2, BGLAP, and CDKN2A genes were further hypomethylated in the BMSC and that of the PPARγ2 gene in the ATSC.

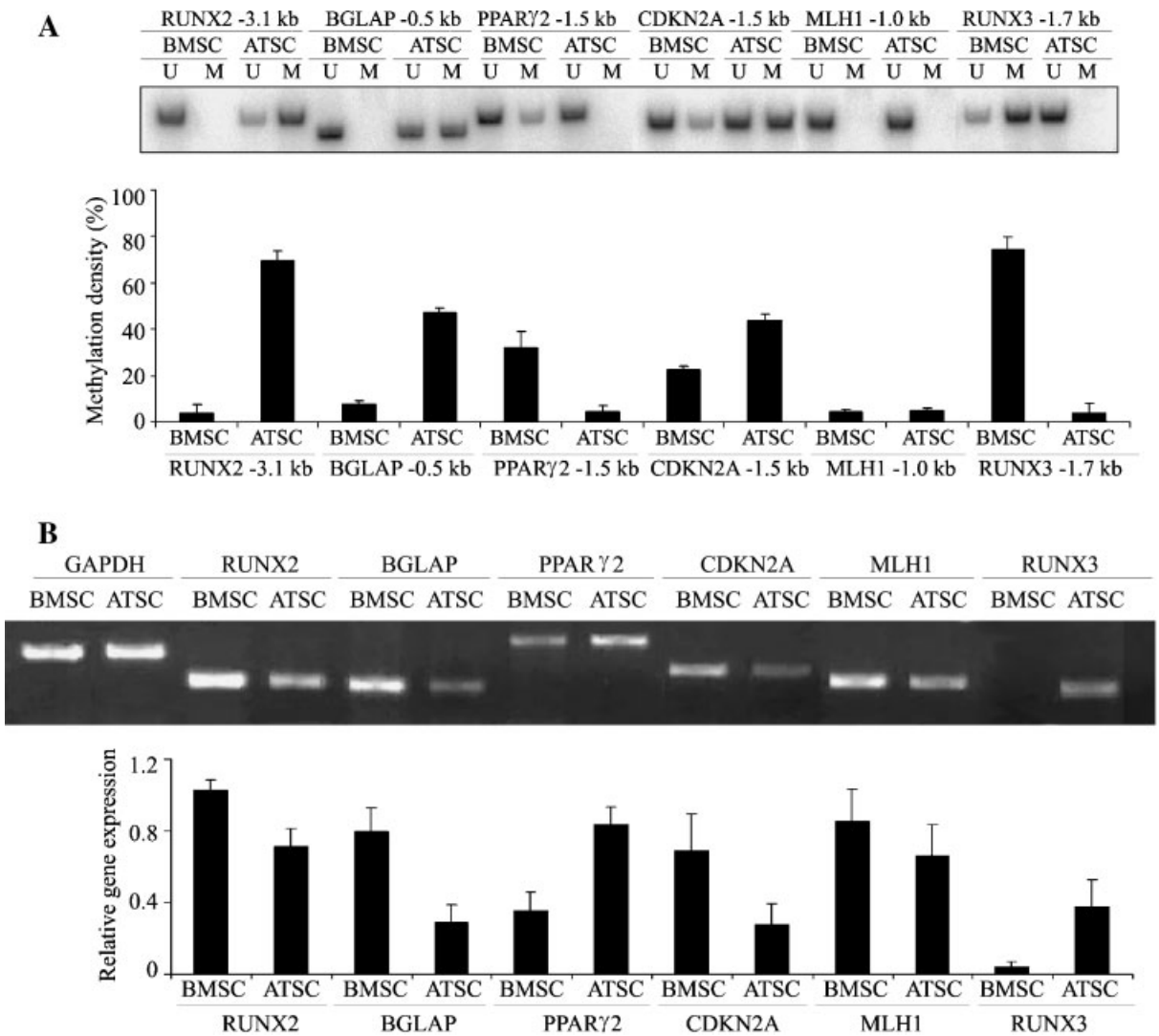

Fig. 4. Transitional CpG methylation and mRNA expression of the six genes in the undifferentiated stromal cells of bone marrows (BMSC) and adipose tissue (ATSC). **A**: A methylation-specific PCR assay was performed using bisulfite-modified genomic DNAs from the primary cultures of three samples. The density of methylation (%) was calculated by the proportion of methylation in a total band intensity of the methylation (M) and unmethylation (U) PCR primers. The genomic position of each CpG amplicon is indicated by the gene symbol and the distance (kb nucleotides) from the transcription start site. **B**: The total RNAs were obtained from the primary cultures of three samples. The signal intensity of the reverse-transcription PCR band was measured and normalized with respect to that of endogenous GAPDH. Columns represent the mean level standard deviation of three samples. Tables I and II list all information about the methylationspecific and reverse-transcription PCR primers.

The mRNA expression of the RUNX2 and RUNX3 genes were examined in exons 1 and 2, which were derived from the P2 promoter regions. The hypomethylation of the methylation-variable CpGs in the BMSC and ATSC tended to coincide with the higher levels of corresponding gene expression (Fig. 4B). Complete hypermethylation of the transitional CpGs area was observed at −1.0-kb CpG site of the RUNX3 gene with no mRNA expression in the BMSC and at −1.9-kb CpG site of the RUNX2 gene with a weak level of mRNA expression in the ATSC (Figs. 3A and 4B). The MLH1 gene demonstrated transitional CpGs that were completely hypomethylated in both the BMSC and ATSC. However, MLH1 expression was higher in the BMSC than in the ATSC.

Effect of Differentiation Induction on Methylation-Variable CpGs and Gene Expression

The primary cultures of both BMSC and ATSC were subcultured in the osteogenic and

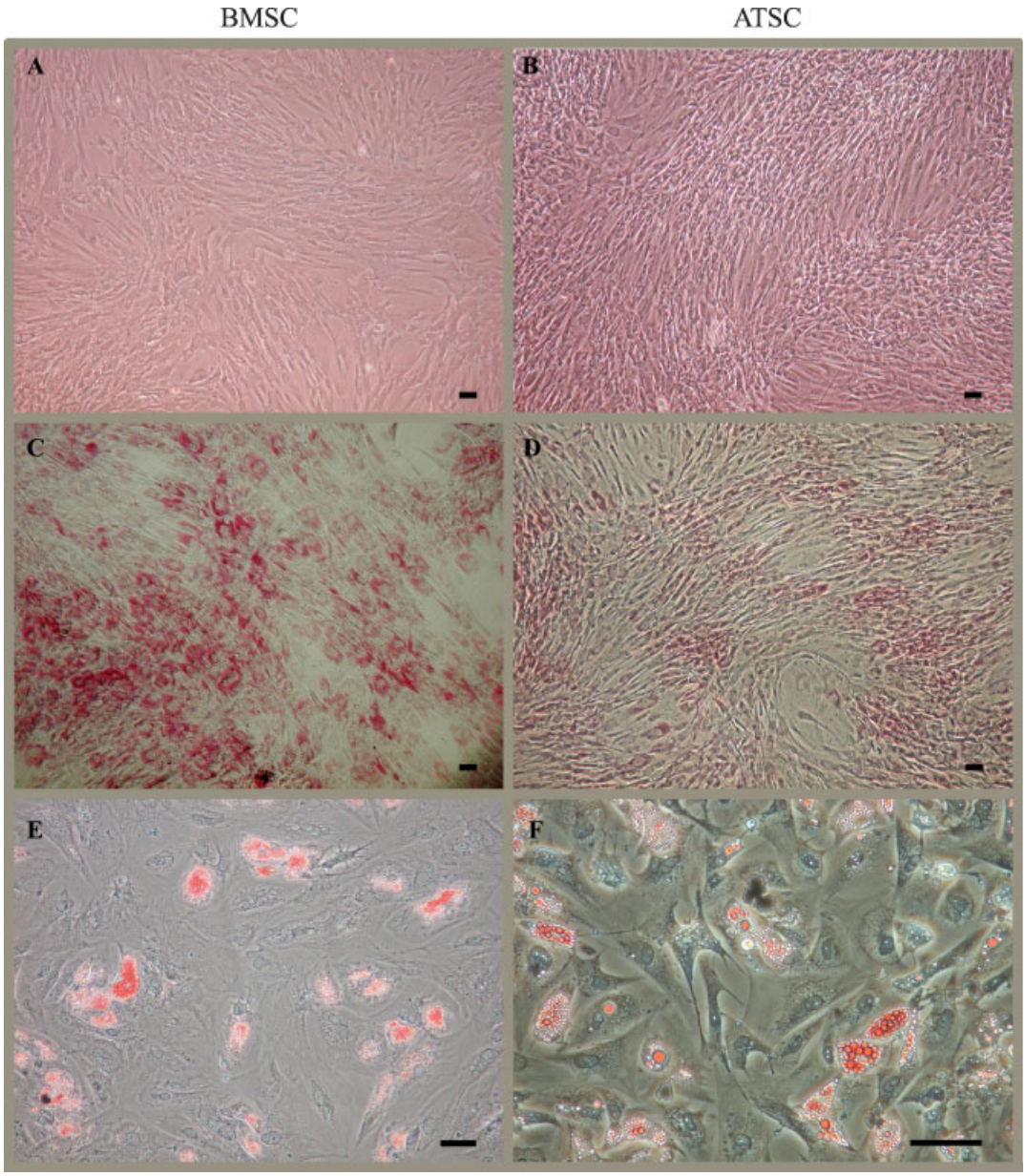

Fig. 5. Inverted optical microscopic pictures of the bone marrow-derived (BMSC) and adipose tissue-derived (ATSC) stromal cells. The BMSC and ATSC were observed with special stain of osteogenic and adipogenic differentiation. The undifferentiated BMSC (**A**) and ATSC (**B**) show a similarly elongated fibroblastic morphology. The osteogenic differentiation of BMSC (**C**) and ATSC (**D**) shows pink colored cytoplasm in the alkaline phosphatase histochemical stain. The adipogenic differentiation of BMSC (**E**) and ATSC (**F**) shows red colored lipid droplets in the Oil Red O stain. Scale bar, 100 μm.

adipogenic media for 2 weeks (Fig. 5). The alkaline phosphatase activity was induced by the osteogenic induction of the BMSC and ATSC, as confirmed by the histochemical staining. Both BMSC and ATSC grown in the adipogenic media showed changes from an elongated fibroblastic appearance to a rounder shape, and were stained positively with Oil Red O, an established lipid dye.

An analysis of methylation-variable CpGs showed the following (Fig. 6A): (i) the tissue-specific methylation of the RUNX2 and BGLAP genes did not change with the osteogenic and adipogenic induction of both BMSC and ATSC, (ii) the incompletely hypomethylated CpG sites

of the PPARγ2 and CDKN2A genes in the BMSC became completely hypomethylated with osteogenic induction, (iii) the intermediately methylated CpGs of the CDKN2A gene in the ATSC become further hypermethylated with both the osteogenic and adipogenic induction, and (iv) the completely hypomethylated CpGs of the genes examined did not change with both the osteogenic and adipogenic induction.

RT-PCR analysis revealed a greater than equal to twofold increase or decrease in the mRNA expression of the PPARγ2 and BGLAP genes as follows (Fig. 6B): (i) the expression of the PPARγ2 gene in the BMSC and ATSC increased as a result of osteogenic and adipogenic induction, (ii) the increased mRNA level of the PPARγ2 gene in the ATSC was higher with adipogenic induction than with osteogenic induction, and (iii) BGLAP expression in the BMSC decreased considerably with adipogenic induction. The differentiation induction showed a $\geq$1.5-fold increase in gene expression as follows: (i) the adipogenic induction of the ATSC increased RUNX2 expression and (ii) CDKN2A expression in the BMSC and MLH1 expression in the BMSC and ATSC were different between the osteogenic induction that increased expression and the adipogenic induction that decreased expression. The PPARγ2 and MLH1 genes showed a similar RT-PCR intensity in the control BMSC and ATSC grown in the secondary cultures.

Effect of Oxidative Stress on Transitional CpG Methylation

The 4-week or 5-week cultured stromal cells were exposed to various doses of H_2O_2, 0.1 mM, 0.3 mM, and 0.5 mM, for 24 h. The transitional methylation of each gene was measured 1 week after the H_2O_2 treatment. H_2O_2 reduced the number of cells in the ATSC cultures considerably at all doses tested (Fig. 7A), which generated detectable CpG amplicon signals in MSP analysis using a radioisotope but no detectable RT-PCR signals.

An analysis of the transitional CpGs showed the following (Fig. 7B): (i) the transitional methylation of the PPARγ2 and CDKN2A genes in the BMSC culture decreased linearly according to the H_2O_2 dose, (ii) the transitional methylation of the CDKN2A gene in the ATSC culture was hypomethylated to various degrees, and (iii) methylation-variable CpGs of the RUNX2, BGLAP, and RUNX3 genes in both BMSC and ATSC cultures did not change after the H_2O_2 treatment. The expression of the six genes in the BMSC did not change at all H_2O_2 doses tested (data not shown).

DISCUSSION

Despite the large number of reports on the relationship between the CpG islands and gene expression, the length and location of CpG islands are so heterogeneous that the extent and boundary of CpG methylation influencing gene expression cannot be explained in a simple manner [Jones, 1999]. In this study, a long CpG island of the osteoblast-specific RUNX2 gene was completely hypomethylated in the BMSC. The nonisland CpG site close to the transcription start site of the osteoblast-specific BGLAP gene was also completely hypomethylated in the BMSC. The distal boundary of the CpG islands upstream of the adipocyte-specific PPARγ2 gene in the ATSC was completely hypomethylated. These complete hypomethylation levels observed in the CpG island boundary or the nonisland CpG site close to the transcription start site were consistent with the high expression levels. These genes in the counterpart cells showed higher levels of methylation at the same CpG sites and lower levels of expression. This suggests a general trend where the transitional CpGs chosen are more methylated when the gene is less expressed and less methylated when the gene is more expressed (Table III).

Complete hypermethylation at −1.9-kb CpG site (P2 promoter) of the RUNX2 was accompanied by a weak level of mRNA derived from P2 promoter in the ATSC (Figs. 3A and 4B). The RUNX3 gene is associated with the development of the gastric mucosa [Li et al., 2002]. The proximal part (−1.0 kb, P2 promoter) of the RUNX3 CpG island was completely hypermethylated in the BMSC showing no mRNA derived from the P2 promoter and incompletely hypermethylated in the ATSC showing weak mRNA expression (Fig. 3). This indicates that complete gene silencing can result from complete CpG island hypermethylation at a CpG site of −1 kb.

Lineage-specific DNA methylation established at the initial embryonic stage is stably maintained during an individual's lifetime [Ahuja and Issa, 2000; Issa, 2000]. Accordingly, in this study, there were no notable changes in the transitional CpG methylation and gene

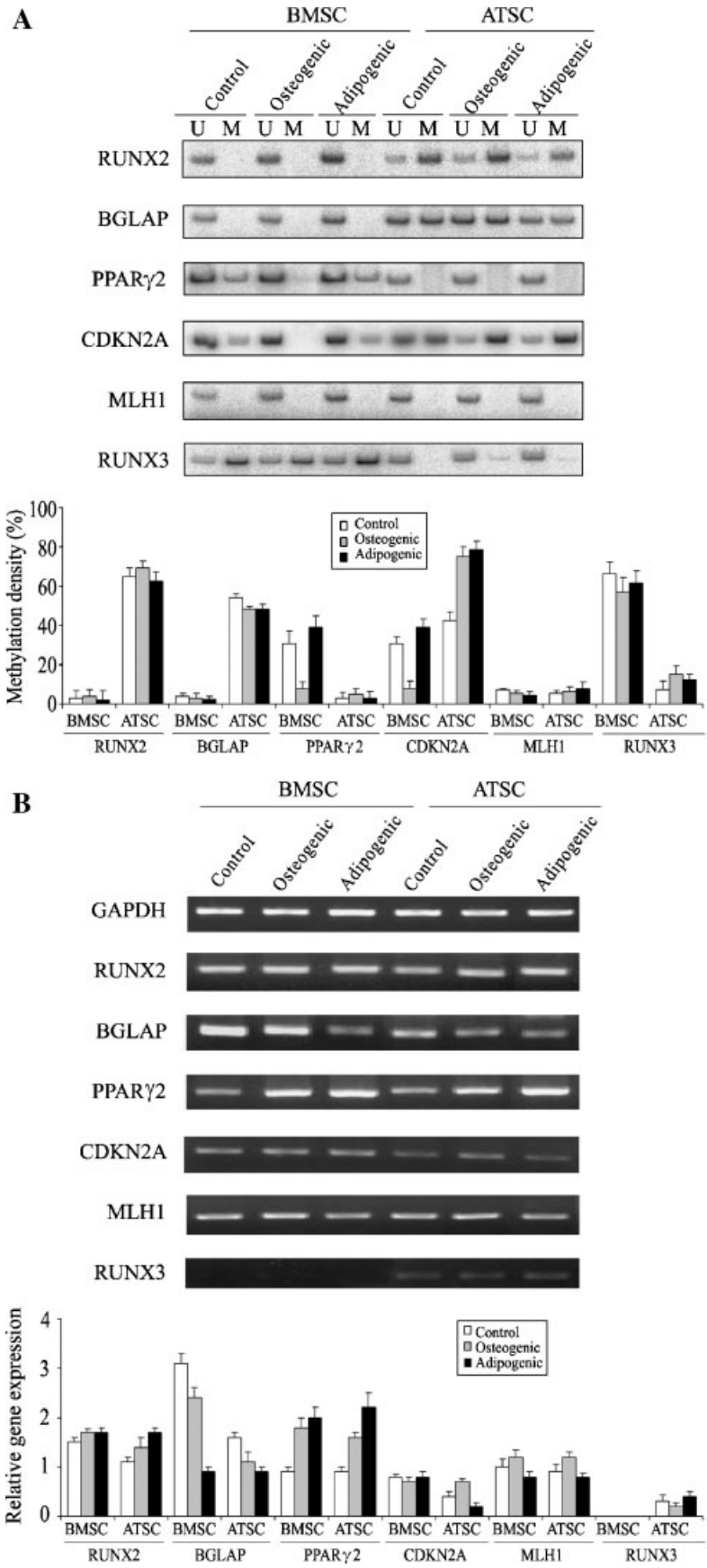
A
BMSC
ATSC
Control
Osteogenic
Adipogenic
U M
RUNX2
BGLAP
PPARγ2
CDKN2A
MLH1
RUNX3
Methylation density (%)
Control
Osteogenic
Adipogenic
BMSC ATSC
B
GAPDH
Relative gene expression

Fig. 6.

expression after the induction of differentiation, or only slight differences in the methylation status between the different differentiation inductions. However, the transitional CpGs of the PPARγ2 gene in the BMSC were hypomethylated after the osteoblast differentiation, and those of the CDKN2A gene in the ATSC were hypermethylated after the adipocyte differentiation (Table III). The spread of DNA methylation is not static, but instead varies at individual CpG sites in the same-type cells (Fig. 7). A wide spectrum of variously methylated alleles in the transitional area is believed to reach a dynamic equilibrium in a given tissue environment [Turker, 2002]. It is possible that a subset of stromal cells predominantly expand in response to cell-external stimulation, leading to methylation alterations. The transitional area of the PPARγ2 and CDKN2A genes was closely bordered by the L1 or LTR elements, whereas the long CpG islands of the RUNX2 and RUNX3 genes that showed insignificant methylation and expression alterations neighbored a few retroelements (Fig. 1). Because the L1 elements can initiate the long-distance spread of tissue-specific methylation [Kang et al., 2006; Kim et al., 2006], the L1-associated CpGs in the transitional area of the PPARγ2 and CDKN2A gene are likely to be often related to methylation alterations.

There are well-known clinical conditions that predispose BMSC to adipogenesis. Avascular necrosis of the hips is associated with the long-term use of steroids as well as with a fat embolism [Chang et al., 1993; Assouline-Dayan et al., 2002]. Glucocorticoid-induced bone loss increases the level of adipogenesis and decreases the level of osteogenesis in the bone marrow [Mazziotti et al., 2006]. Oxidative stress is believed to link aging and age-related osteoporosis [Basu et al., 2001]. As a person ages, the fat content of the bone marrow increases and forms a more yellow marrow [Justesen et al., 2001; Pei and Tontonoz, 2004]. In this study, the PPARγ2 gene in the BMSC was bordered by incompletely hypomethylated transitional CpGs, which were completely hypomethylated after exposure to the steroid-containing media and a H_2O_2 treatment. Weak transitional methylation of the PPARγ2 gene in the bone marrow environment is likely to be prone to complete hypomethylation, suggesting that a methylation-dependent mechanism is involved in senile as well as steroid-induced osteoporosis.

Weak transitional methylation of the PPARγ2 gene in the BMSC became hypomethylated during osteogenic induction but not during adipogenic induction (Fig. 6A). The transitional CpGs of the PPARγ2 gene were hypomethylated in a manner independent of the steroid dose in the culture media, because the steroid dose was higher in the adipogenic medium than in the osteogenic medium. With respect to methylation kinetics, the reestablishment of methylation on a newly replicated DNA strand is needed in order to continue cell-specific gene expression in the subsequent cell cycle. A strong link between the timing of transcription and replication provides opportunities for maintaining the level of DNA methylation [Schubeler et al., 2002; Woodfine et al., 2004]. Most cells in the heterogeneous methylation state synchronously enter the cell cycle and go through one or two rounds of cell division before differentiating [Tseng et al., 2005]. The in vitro osteogenic induction appears to initiate newly synchronized expansion, and further increase the proportion of the BMSC containing the hypomethylated transitional CpGs of the PPARγ2 gene.

The transitional CpGs of the CDKN2A gene, which were intermediately methylated in the ATSC, were further hypermethylated during both osteogenic and adipogenic induction. The RT-PCR results showed a high CDKN2A expression in BMSC and a low CDKN2A expression in ATSC. Previous studies reported that the proliferation and differentiation of mesenchymal cells was differentially checked by the CDKN2A (BMSC) and E2F (ATSC) cell

Fig. 6. Transitional CpG methylation and expression profiles of the six genes examined in the stromal cells derived from bone marrow (BMSC) and adipose tissue (ATSC). Both BMSC and ATSC were grown in the standard media for 4 or 5 weeks and subcultured in the osteogenic or adipogenic supplements. The undifferentiated stromal cells for the control experiments were grown in a standard medium for the same culture period. The BMSC and ATSC were examined by both methylation-specific (**A**) and reversetranscription (**B**) PCR analyses. The methylation status of the transitional CpGs is reported as the mean percentage of methylated CpGs estimated from the PCR bands amplified by the methylation (M) and unmethylation (U) primers. The intensity of the reverse-transcription PCR band was measured and normalized with respect to that of the endogenous GAPDH. Columns represent the mean level standard deviation of the results of three samples in each culture condition.

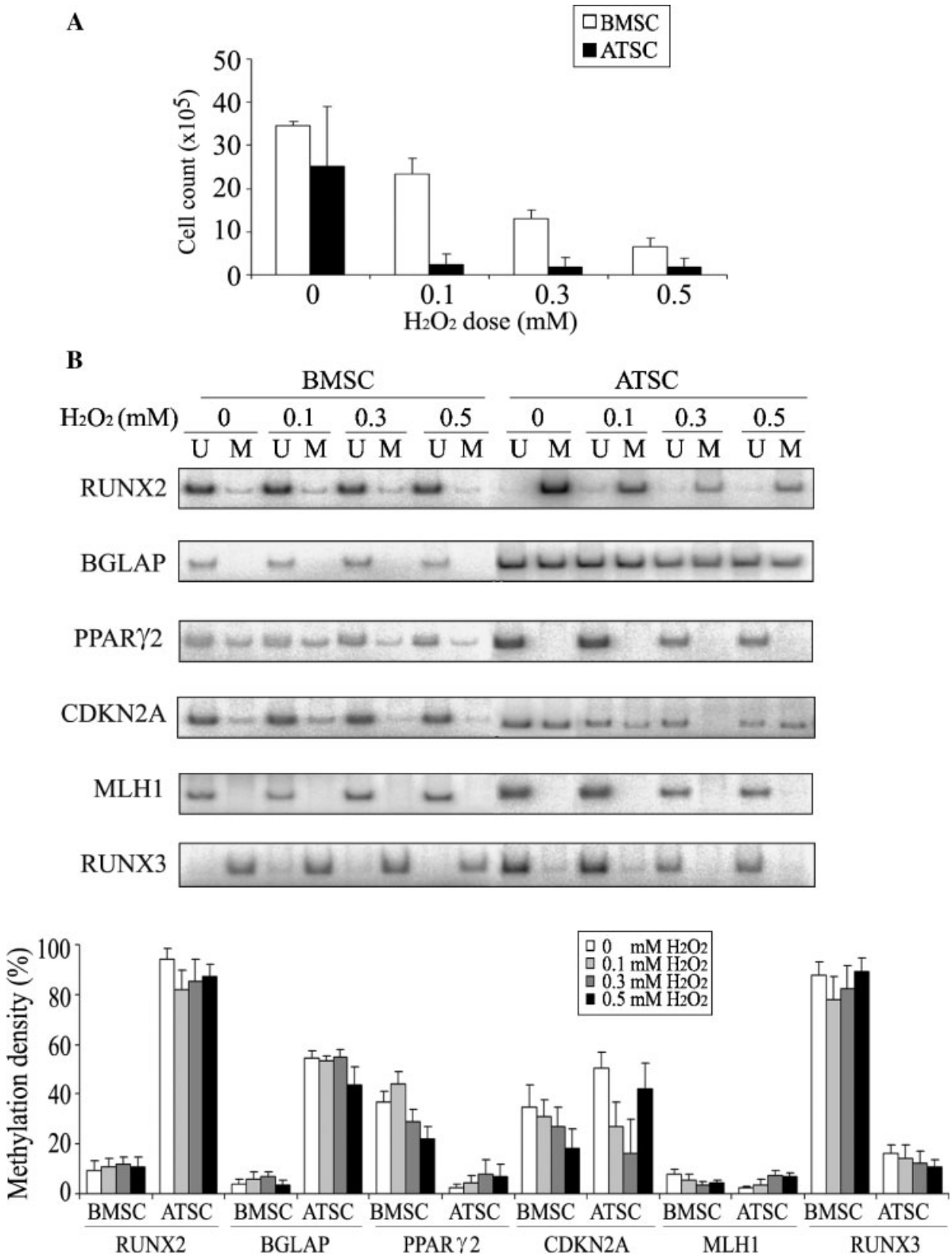

Fig. 7. Transitional CpG methylation of the six genes examined in the bone marrow (BMSC)- and adipose tissue (ATSC)-derived stromal cells treated with H_2O_2. **A**: The number of cells was counted 1 week after exposing the BMSC and ATSC to H_2O_2. **B**: The methylation status of the transitional CpGs is reported as the mean percentage of methylated CpGs estimated from the PCR bands amplified by the methylation (M) and unmethylation (U) primers. Columns represent the mean methylation level standard deviations of three samples.

TABLE III. Relationships Between Transitional CpG Methylation and Gene Expression in Mesenchymal Cells[a]

	Predifferentiation				Differentiation			
	Marrow		Fat		Marrow		Fat	
	MSP	RT-PCR	MSP	RT-PCR	MSP	RT-PCR	MSP	RT-PCR
Tissue-specific genes								
RUNX2	−	+++	+++	++	−	+++	+++	+++
BGLAP	−	++++	++	++	−	+++	++	+
PPARγ2	+	+	−	+++	−	+++	−	++++
RUNX3	++++	−	+++	+	++++	−	+++	+
Housekeeping genes								
CDKN2A	+	++	++	+	−	++	+++	+
MLH1	−	++	−	+	−	++	−	++

[a]MSP, methylation-specific PCR. The methylation status of the methylation-variable CpGs was divided into the following five levels: (0–20%, −; 21–40%, +; 41–60%, ++; 61–80%, +++; 81–100%, ++++). RT-PCR, reverse-transcription PCR. The RT-PCR results in Figures 4 and 6 were divided into five levels; strong PPARγ2 expression in differentiated adipocytes and bone-specific BGLAP expression (++++), bone-specific RUNX2 and fat-specific PPARγ2 expression (+++), housekeeping CDKN2A and MLH1 expression (++), weak expression in counterpart cell type (+), and silenced RUNX2 (−) gene in the marrow.

cycle regulators [Oliva et al., 2003; Miard and Fajas, 2005]. This suggests that the CDKN2A gene can be suppressed by transitional hypermethylation during the differentiation of ATSC under the control of the E2F cell cycle regulators.

The BMSC treated with H_2O_2 showed hypomethylation alterations in the transitional CpGs of the PPARγ2 and CDKN2A genes in proportion to the H_2O_2 dose added to the BMSC culture. The number of cells in the ATSC cultures decreased considerably after the H_2O_2 treatment compared with that of the BMSC culture (Fig. 7A). The ATSC treated with H_2O_2 showed hypomethylation at various levels in the transitional CpGs of the CDKN2A gene (Fig. 7B). A previous study reported that low doses of reactive oxygen species stimulate cell proliferation, but high doses cause cellular damage and cell cycle arrest [Yoon et al., 2002]. It is possible that the transitional CpGs of the CDKN2A gene are hypermethylated in a small proportion of BMSC and a large fraction of ATSC, which undergo cell death and cell cycle arrest due to a susceptibility to oxidative stress. Consequently, most of the viable cells resistant to the H_2O_2 treatment are likely to contain the hypomethylated alleles of the PPARγ2 and CDKN2A genes.

The adipocyte-specific PPARγ2 gene in the BMSC showed transitional CpGs hypomethylation and increased expression after the osteogenic differentiation. The expression of the PPARγ2 gene might be enhanced in the osteogenic media enriched in lineage-specific factors. The expression of the osteoblast-specific RUNX2 gene did not change in the osteogenic media. A previous study reported that the RUNX2 expression can be increased on a substrate culture mimicking a tissue environment such as lamin, fibronectin, and collagen [Cool and Nurcombe, 2005]. The RUNX2 gene having two promoters is believed to autoregulated by negative feedback on their own promoters to stringently control gene expression in a tissue environment [Ogawa et al., 1993; Stewart et al., 1997; Xiao et al., 2003].

In conclusion, a section of hypomethylated CpGs in the transitional area between promoters and retroelements is associated with increased gene expression in mesenchymal cells. Mesenchymal cells withstand the tissue-specific methylation of transitional CpGs under the in vitro induction of differentiation. It is suggested that mesenchymal cells can transiently shift from one position to another largely dependent on the lineage-specific factors added to the culture media. This provides important information for stem cell therapy, which is still a highly experimental procedure that has not yet reached clinical applications. Interestingly, the weak transitional CpG methylation of the adipocyte-specific PPARγ2 gene in BMSC was prone to hypomethylation under osteogenic induction and oxidative stress, suggesting the involvement of a methylation-dependent mechanism in the adipogenesis of bone marrow.

REFERENCE

Ahuja N, Issa JP. 2000. Aging, methylation and cancer. Histol Histopathol 15:835–842.

Arnaud P, Goubely C, Pelissier T, Deragon JM. 2000. SINE retroposons can be used in vivo as nucleation centers for de novo methylation. Mol Cell Biol 20:3434–3441.

Assouline-Dayan Y, Chang C, Greenspan A, Shoenfeld Y, Gershwin ME. 2002. Pathogenesis and natural history of osteonecrosis. Semin Arthritis Rheum 32:94–124.

Bangsow C, Rubins N, Glusman G, Bernstein Y, Negreanu V, Goldenberg D, Lotem J, Ben Asher E, Lancet D, Levanon D, Groner Y. 2001. The RUNX3 gene-sequence, structure and regulated expression. Gene 279:221–232.

Basu S, Michaelsson K, Olofsson H, Johansson S, Melhus H. 2001. Association between oxidative stress and bone mineral density. Biochem Biophys Res Commun 288: 275–279.

Bird AP. 1986. CpG-rich islands and the function of DNA methylation. Nature 321:209–213.

Chang CC, Greenspan A, Gershwin ME. 1993. Osteonecrosis: Current perspectives on pathogenesis and treatment. Semin Arthritis Rheum 23:47–69.

Cool SM, Nurcombe V. 2005. Substrate induction of osteogenesis from marrow-derived mesenchymal precursors. Stem Cells Dev 14:632–642.

Dennis JE, Charbord P. 2002. Origin and differentiation of human and murine stroma. Stem Cells 20:205–214.

Gardiner-Garden M, Frommer M. 1987. CpG islands in vertebrate genomes. J Mol Biol 196:261–282.

Hata K, Sakaki Y. 1997. Identification of critical CpG sites for repression of L1 transcription by DNA methylation. Gene 189:227–234.

Holliday R, Pugh JE. 1975. DNA modification mechanisms and gene activity during development. Science 187:226–232.

Hong SJ, Kim YH, Choi YD, Min KO, Choi SW, Rhyu MG. 2005. Relationship between the extent of chromosomal losses and the pattern of CpG methylation in gastric carcinomas. J Korean Med Sci 20:790–805.

Issa JP. 2000. The epigenetics of colorectal cancer. Ann NY Acad Sci 910:140–153.

Jones PA. 1999. The DNA methylation paradox. Trends Genet 15:34–37.

Jurka J. 2000. Repbase update: A database and an electronic journal of repetitive elements. Trends Genet 16:418–420.

Justesen J, Stenderup K, Ebbesen EN, Mosekilde L, Steiniche T, Kassem M. 2001. Adipocyte tissue volume in bone marrow is increased with aging and in patients with osteoporosis. Biogerontology 2:165–171.

Kang MI, Rhyu MG, Kim YH, Jung YC, Hong SJ, Cho CS, Kim HS. 2006. The length of CpG islands is associated with the distribution of Alu and L1 retroelements. Genomics 87:580–590.

Kern S, Eichler H, Stoeve J, Kluter H, Bieback K. 2006. Comparative analysis of mesenchymal stem cells from bone marrow, umbilical cord blood, or adipose tissue. Stem Cells 24:1294–1301.

Kim YH, Hong SJ, Jung YC, Kim SJ, Seo EJ, Choi SW, Rhyu MG. 2006. The 5'-end transitional CpGs between the CpG islands and retroelements are hypomethylated in association with loss of heterozygosity in gastric cancer. BMC Cancer 6:180.

Komori T, Yagi H, Nomura S, Yamaguchi A, Sasaki K, Deguchi K, Shimizu Y, Bronson RT, Gao YH, Inada M, Sato M, Okamoto R, Kitamura Y, Yoshiki S, Kishimoto T. 1997. Targeted disruption of Cbfa1 results in a complete lack of bone formation owing to maturational arrest of osteoblasts. Cell 89:755–764.

Larsen F, Gundersen G, Lopez R, Prydz H. 1992. CpG islands as gene markers in the human genome. Genomics 13:1095–1107.

Li QL, Ito K, Sakakura C, Fukamachi H, Inoue K, Chi XZ, Lee KY, Nomura S, Lee CW, Han SB, Kim HM, Kim WJ, Yamamoto H, Yamashita N, Yano T, Ikeda T, Itohara S, Inazawa J, Abe T, Hagiwara A, Yamagishi H, Ooe A, Kaneda A, Sugimura T, Ushijima T, Bae SC, Ito Y. 2002. Causal relationship between the loss of RUNX3 expression and gastric cancer. Cell 109:113–124.

Mazziotti G, Angeli A, Bilezikian JP, Canalis E, Giustina A. 2006. Glucocorticoid-induced osteoporosis: An update. Trends Endocrinol Metab 17:144–149.

Miard S, Fajas L. 2005. Atypical transcriptional regulators and cofactors of PPARgamma. Int J Obes (Lond) 29 (Suppl 1):S10–S12.

Ogawa E, Maruyama M, Kagoshima H, Inuzuka M, Lu J, Satake M, Shigesada K, Ito Y. 1993. PEBP2/PEA2 represents a family of transcription factors homologous to the products of the Drosophila runt gene and the human AML1 gene. Proc Natl Acad Sci USA 90:6859–6863.

Oliva A, Borriello A, Zeppetelli S, Di Feo A, Cortellazzi P, Ventriglia V, Criscuolo M, Zappia V, Della RF. 2003. Retinoic acid inhibits the growth of bone marrow mesenchymal stem cells and induces p27Kip1 and p16INK4A up-regulation. Mol Cell Biochem 247:55–60.

Otto F, Thornell AP, Crompton T, Denzel A, Gilmour KC, Rosewell IR, Stamp GW, Beddington RS, Mundlos S, Olsen BR, Selby PB, Owen MJ. 1997. Cbfa1, a candidate gene for cleidocranial dysplasia syndrome, is essential for osteoblast differentiation and bone development. Cell 89:765–771.

Pei L, Tontonoz P. 2004. Fat's loss is bone's gain. J Clin Invest 113:805–806.

Reik W, Dean W, Walter J. 2001. Epigenetic reprogramming in mammalian development. Science 293:1089–1093.

Ross SR, Graves RA, Greenstein A, Platt KA, Shyu HL, Mellovitz B, Spiegelman BM. 1990. A fat-specific enhancer is the primary determinant of gene expression for adipocyte P2 in vivo. Proc Natl Acad Sci USA 87:9590–9594.

Schubeler D, Scalzo D, Kooperberg C, van Steensel B, Delrow J, Groudine M. 2002. Genome-wide DNA replication profile for Drosophila melanogaster: A link between transcription and replication timing. Nat Genet 32:438–442.

Shiota K. 2004. DNA methylation profiles of CpG islands for cellular differentiation and development in mammals. Cytogenet Genome Res 105:325–334.

Stewart M, Terry A, Hu M, O'Hara M, Blyth K, Baxter E, Cameron E, Onions DE, Neil JC. 1997. Proviral insertions induce the expression of bone-specific isoforms of PEBP2alphaA (CBFA1): Evidence for a new myc collaborating oncogene. Proc Natl Acad Sci U S A 94:8646–8651.

Tontonoz P, Hu E, Graves RA, Budavari AI, Spiegelman BM. 1994. mPPAR gamma 2: Tissue-specific regulator of an adipocyte enhancer. Genes Dev 8:1224–1234.

Tseng YH, Butte AJ, Kokkotou E, Yechoor VK, Taniguchi CM, Kriauciunas KM, Cypess AM, Niinobe M, Yoshikawa K,

Patti ME, Kahn CR. 2005. Prediction of preadipocyte differentiation by gene expression reveals role of insulin receptor substrates and necdin. Nat Cell Biol 7:601–611.

Turker MS. 2002. Gene silencing in mammalian cells and the spread of DNA methylation. Oncogene 21:5388–5393.

Woodfine K, Fiegler H, Beare DM, Collins JE, McCann OT, Young BD, Debernardi S, Mott R, Dunham I, Carter NP. 2004. Replication timing of the human genome. Hum Mol Genet 13:191–202.

Xiao ZS, Simpson LG, Quarles LD. 2003. IRES-dependent translational control of Cbfa1/Runx2 expression. J Cell Biochem 88:493–505.

Yates PA, Burman RW, Mummaneni P, Krussel S, Turker MS. 1999. Tandem B1 elements located in a mouse methylation center provide a target for de novo DNA methylation. J Biol Chem 274:36357–36361.

Yoon SO, Yun CH, Chung AS. 2002. Dose effect of oxidative stress on signal transduction in aging. Mech Ageing Dev 123:1597–1604.

Zhu Y, Qi C, Korenberg JR, Chen XN, Noya D, Rao MS, Reddy JK. 1995. Structural organization of mouse peroxisome proliferator-activated receptor gamma (mPPAR gamma) gene: Alternative promoter use and different splicing yield two mPPAR gamma isoforms. Proc Natl Acad Sci USA 92:7921–7925.